Acta Crystallographica Section F
Structural Biology and Crystallization Communications
ISSN 1744-3091

Crystallization and diffraction of an Lhx4–Isl2 complex

Morgan S. Gadd, David B. Langley, J. Mitchell Guss and Jacqueline M. Matthews*

School of Molecular and Microbial Biosciences, University of Sydney, Australia

Correspondence e-mail: j.matthews@usyd.edu.au

Received 21 October 2008
Accepted 20 December 2008

A stable intramolecular complex comprising the LIM domains of the LIM-homeodomain protein Lhx4 tethered to a peptide region of Isl2 has been engineered, purified and crystallized. The monoclinic crystals belonged to space group $P2_1$, with unit-cell parameters $a = 46.8$, $b = 88.7$, $c = 49.9$ Å, $\beta = 111.9^\circ$, and diffracted to 2.16 Å resolution.

1. Introduction

LIM-homeodomain (LIM-HD) transcription factors are essential for the developmental processes of many tissues (Hunter & Rhodes, 2005). LIM-HD proteins comprise a pair of N-terminal LIM domains, a centrally located homeodomain and poorly characterized C-terminal sequences. LIM domains are composed of tandem zinc-finger motifs and mediate protein–protein interactions; the acronym is derived from the three genes in which the domain was first identified: *lin-11*, *isl-1* and *mec-3* (Bach, 2000; Way & Chalfie, 1988; Freyd *et al.*, 1990; Karlsson *et al.*, 1990). The homeodomains of LIM-HD proteins bind specific AT-rich sites in DNA.

Many LIM-HDs have been implicated in the development of the central nervous system (for a recent review, see Bachy *et al.*, 2002). In particular, Lhx3 and Isl1 are known to specify distinct cell types in the developing ventral neural cord. A direct interaction between the LIM domains of Lhx3 and the C-terminal region of Isl1 is necessary for motor-neuron development (Jurata *et al.*, 1998; Thaler *et al.*, 2002). The Lhx3-binding domain (LBD) of Isl1 was defined as residues 262–291 and was found to bind Lhx3 in a manner similar to that of the LIM-interaction domain of LIM domain-binding protein 1 (Ldb1; Bhati, Lee, Nancarrow, Lee *et al.*, 2008), which interacts with all LIM-HD proteins (reviewed in Matthews & Visvader, 2003). Indeed, in motor neurons Isl1 is able to displace Lhx3 as the binding partner of Ldb1 by providing Lhx3 with the decoy interaction domain.

In terms of sequence similarity, Lhx4 is the LIM-HD family member that is most closely related to Lhx3 (protein sequence identity of 62%) and Isl2 is most closely related to Isl1 (protein sequence identity of 75%). Both Lhx4 and Isl2 are also expressed in motor neurons. Lhx4 has been shown to be redundant with Lhx3 for motor-neuron specification, suggesting that it may mediate a similar interaction with Isl1 (Sharma *et al.*, 1998). Isl2 has been shown to bind Lhx3 *via* its C-terminal domain (Jurata *et al.*, 1998). Residues 272–301 of Isl2 have 60% sequence identity with the LBD of Isl1.

Previously, we have determined crystal structures of engineered proteins comprising the LIM domains of the LIM-only protein LMO4 in complex with Ldb1 (PDB code 1rut) and of Lhx3 in complex with Isl1 (PDB code 2rgt), as well as the solution structure of Lhx3 in complex with Ldb1 (PDB code 2jtn) (Bhati, Lee, Nancarrow, Lee *et al.*, 2008; Deane *et al.*, 2004). The LIM domains in these complexes have 41% and 81% sequence identity to the LIM domains of Lhx4, respectively. Owing to the redundancy of the proteins involved in motor-neuron specification, we surmised that Isl2 might also interact with Lhx4. Here, we report the successful purification and crystallization of an engineered complex comprising the LIM domains of Lhx4 and the LBD of Isl2 and present preliminary analysis of the diffraction data obtained.

2. Methods

2.1. Cloning, expression and purification

A construct containing residues 24–159 of murine Lhx4 (NCBI entry NP_034842), a linker encoding GGSGGHMGSGG and residues 272–301 of Isl2 (NCBI entry NP_081673) was cloned into a pGEX-2T vector (GE Healthcare), which allows the protein to be expressed with an N-terminal glutathione *S*-transferase (GST) tag. The resulting plasmid was transformed into *Escherichia coli* BL21 (DE3) cells and protein expression was induced for 20 h by the addition of IPTG to 0.4 m*M* at 293 K in Luria Broth. Cell lysis was achieved by freeze–thawing (three cycles) and sonication in a buffer containing 100 m*M* NaCl, 50 m*M* Tris–HCl pH 8.0, 0.1%(*v*/*v*) β-mercaptoethanol, 0.1%(*v*/*v*) Triton X-100, 1.4 m*M* phenylmethylsulfonyl fluoride, 0.1 mg ml^{-1} lysozyme and 10 µg ml^{-1} DNaseI. After centrifugation, the resulting clarified lysate was applied onto glutathione Sepharose 4B resin (GE Healthcare) for purification by affinity chromatography. The Lhx4–Isl2 complex was eluted by cleavage from the affinity-bound GST tag using thrombin, resulting in two additional residues (GS) at the N-terminus of Lhx4. The tethered complex was further purified by size-exclusion chromatography on a HiLoad 16/60 Superdex-200 column (GE Healthcare) in a buffer containing 20 m*M* Tris–HCl pH 8.0, 150 m*M* NaCl and 1 m*M* dithiothreitol. The purified protein was concentrated with centrifugal filtration devices (Vivaspin 6, GE Healthcare) to a concentration of ~10 mg ml^{-1} in the same buffer prior to crystallization. The protein concentration was determined spectrophotometrically by absorbance at 280 nm (NanoDrop ND-1000 Spectrophotometer, Biolab) using a theoretical extinction coefficient of 18 450 M^{-1} cm^{-1}.

2.2. Crystallization

Preliminary crystallization conditions were discovered using commercial sparse-matrix crystallization screens (Qiagen). A Mosquito positive-displacement liquid-handling robot (TTP LabTech) was used to combine equal volumes (200 nl) of crystallization conditions and protein solution (~10 mg ml^{-1}) suspended above well solutions (75 µl) in 96-well hanging-drop format trays. The trays were incubated at room temperature (~293 K). Crystal optimization was achieved in large-scale hanging-drop experiments in which 2 µl of protein and well solutions were combined with or without 0.45 µl of the solutions from Additive Screen (Hampton Research) and equilibrated against 1 ml well solution at room temperature.

Table 1
Data-collection statistics.

Values in parentheses are for the highest resolution shell.

Wavelength (Å)	1.2819
Space group	$P2_1$
Unit-cell parameters (Å, °)	a = 46.8, b = 88.7, c = 49.9, β = 111.9
Resolution limit (Å)	2.16 (2.20–2.16)
Average mosaicity (°)	1.4
Completeness (%)	98.1 (78.2)
Unique reflections	20385
Redundancy	6.9 (4.8)
$R_{\rm merge}$†	0.084 (0.473)
$\langle I/\sigma(I)\rangle$	14.3 (2.5)

† $R_{\rm merge} = \sum_{hkl}\sum_i |I_i(hkl) - \langle I(hkl)\rangle| / \sum_{hkl}\sum_i I_i(hkl)$.

2.3. Data collection and processing

The crystal was cryoprotected by opening the drop to the air and allowing evaporative desiccation to occur over ~5 min to the extent that crystals of $MgSO_4$ started visibly forming, at which point the protein crystal was removed with a loop and immediately flash-cooled in a nitrogen-gas stream at 100 K. Diffraction data were recorded on the Australian Synchrotron beamline PX1 with a Quantum 315 CCD detector (ADSC). 720 frames were recorded at a distance of 150 mm using an oscillation range of 0.5° and 5 s exposures for each frame. The diffraction data were integrated and scaled using the *HKL*-2000 program package (Otwinowski & Minor, 1997).

3. Results and discussion

A complex comprising the LIM domains of Lhx3 and the LBD of Isl2 was generated. The LIM domains of LIM-HD and related LIM-only proteins tend to aggregate; however, this problem can be overcome by tethering the LIM domains to an interacting peptide (Bhati, Lee, Nancarrow, Bach *et al.*, 2008; Deane *et al.*, 2001). Thus, the LBD of Isl2 was fused to the LIM domains of Lhx4 *via* a flexible 11-residue linker. The tethered Lhx4–Isl2 complex (18 600 Da) was purified to >95% purity as determined by SDS–PAGE with Coomassie staining, generating typical yields of ~7–8 mg protein per litre of culture medium. Initial crystallization screening resulted in small crystals after 5 d under 17 of 576 conditions tried. However, larger crystals arranged as clusters of plates were observed under two conditions: Qiagen Classics Suite condition No. 62 (1.6 *M* magnesium sulfate, 0.1 *M* MES pH 6.5) and $AmSO_4$ Suite condition No. 87 [2 *M* ammonium sulfate, 0.1 *M* MES pH 6.5, 5%(*w*/*v*) PEG 400]. Optimization of Classics Suite condition No. 62 yielded several conditions

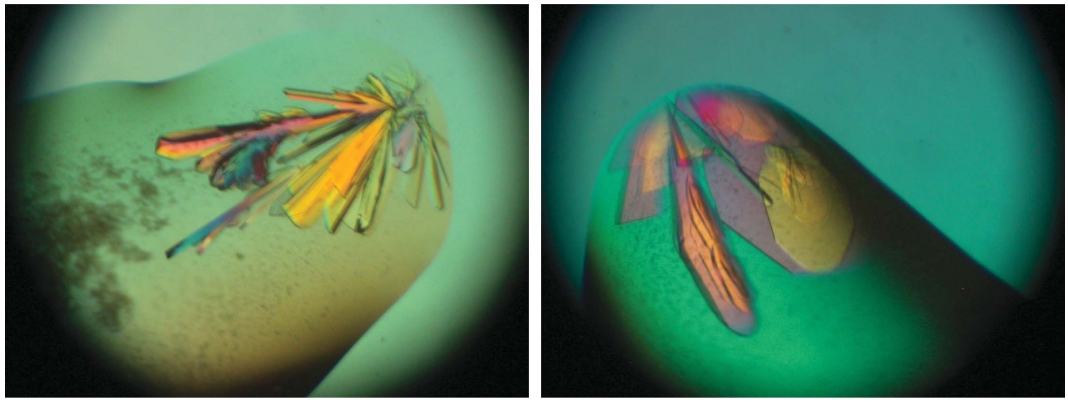

Figure 1
Monoclinic crystals of an Lhx4–Isl2 complex after 14 d incubation. The crystals are ~1 mm in the longest dimension.

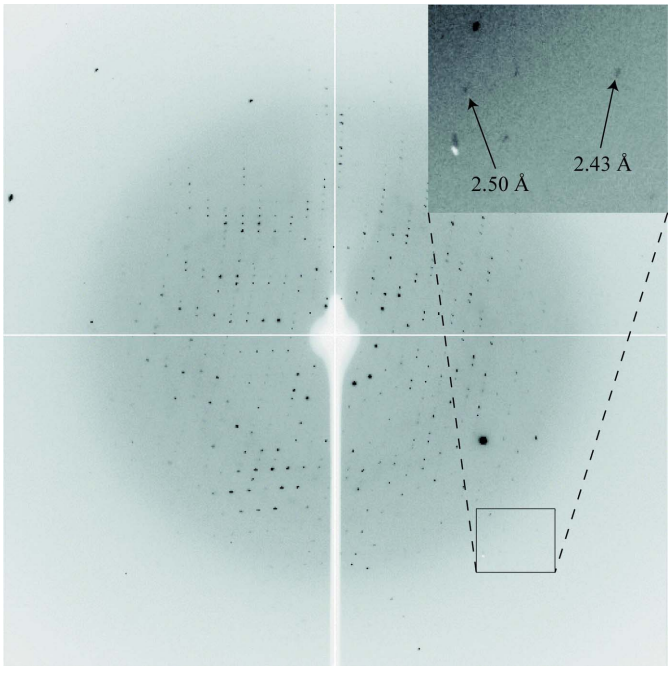

Figure 2
Diffraction image of the Lhx4–Isl2 complex. The inset shows data towards the limit of diffraction (2.16 Å). The image also contains intense reflections resulting from the magnesium sulfate that crystallized during the cryoprotecting process.

that produced stacked plate-shaped crystals of maximum dimension ~1 mm after two weeks: 1.5 *M* magnesium sulfate, 0.1 *M* MES pH 6.5 plus 3%(*w*/*v*) sucrose, 0.01 *M* barium chloride or 0.01 *M* sodium bromide (Fig. 1). Data were recorded from a single crystal that was cut from a crystal cluster grown in 1.5 *M* magnesium sulfate, 0.1 *M* MES pH 6.5, 3%(*w*/*v*) sucrose.

Diffraction data were recorded to 2.16 Å resolution (Fig. 2). Data-collection and processing statistics are summarized in Table 1. The crystals were monoclinic, space group $P2_1$, with unit-cell parameters $a = 46.8$, $b = 88.7$, $c = 49.9$ Å, $\beta = 111.9^\circ$. Two molecules are predicted within the asymmetric unit, resulting in a corresponding specific volume of 2.6 Å^3 Da^{-1} and a solvent content of 52.4% (Matthews, 1968). Calculation of a self-rotation function using *MOLREP* (Vagin & Teplyakov, 1997) reveals a prominent non-origin peak 73% of the magnitude of the origin peak. This peak represents a twofold rotation parallel to the *a* axis of the unit cell. Initial attempts to solve this structure by molecular replacement using the crystal structure of the Lhx3–Isl1 crystal failed, possibly as a result of some flexibility between the domains. Thus, we plan to use the anomalous signal at ~1.28 Å from the eight Zn atoms in the asymmetric unit to obtain experimental phases to solve the structure of the complex.

MSG was supported by an Australian Postgraduate Award. JMM is a Senior Medical Research Fellow of the Viertel Foundation. This work was supported by grant DP663289 from the Australian Research Council. Support to record the diffraction data was provided by the Australian Synchrotron.

References

Bach, I. (2000). *Mech. Dev.* **91**, 5–17.
Bachy, I., Failli, V. & Rétaux, S. (2002). *Neuroreport*, **13**, A23–A27.
Bhati, M., Lee, M., Nancarrow, A. L., Bach, I., Guss, J. M. & Matthews, J. M. (2008). *Acta Cryst.* F**64**, 297–299.
Bhati, M., Lee, C., Nancarrow, A. L., Lee, M., Craig, V. J., Bach, I., Guss, J. M., Mackay, J. P. & Matthews, J. M. (2008). *EMBO J.* **27**, 2018–2029.
Deane, J. E., Ryan, D. P., Sunde, M., Maher, M. J., Guss, J. M., Visvader, J. E. & Matthews, J. M. (2004). *EMBO J.* **23**, 3589–3598.
Deane, J. E., Sum, E., Mackay, J. P., Lindeman, G. J., Visvader, J. E. & Matthews, J. M. (2001). *Protein Eng.* **14**, 493–499.
Freyd, G., Kim, S. K. & Horvitz, H. R. (1990). *Nature (London)*, **344**, 876–879.
Hunter, C. S. & Rhodes, S. J. (2005). *Mol. Biol. Rep.* **32**, 67–77.
Jurata, L. W., Pfaff, S. L. & Gill, G. N. (1998). *J. Biol. Chem.* **273**, 3152–3157.
Karlsson, O., Thor, S., Norberg, T., Ohlsson, H. & Edlund, T. (1990). *Nature (London)*, **344**, 879–882.
Matthews, B. W. (1968). *J. Mol. Biol.* **33**, 491–497.
Matthews, J. M. & Visvader, J. E. (2003). *EMBO Rep.* **4**, 1132–1137.
Otwinowski, Z. & Minor, W. (1997). *Methods Enzymol.* **276**, 307–326.
Sharma, K., Sheng, H. Z., Lettieri, K., Li, H., Karavanov, A., Potter, S., Westphal, H. & Pfaff, S. L. (1998). *Cell*, **95**, 817–828.
Thaler, J. P., Lee, S. K., Jurata, L. W., Gill, G. N. & Pfaff, S. L. (2002). *Cell*, **110**, 237–249.
Vagin, A. & Teplyakov, A. (1997). *J. Appl. Cryst.* **30**, 1022–1025.
Way, J. C. & Chalfie, M. (1988). *Cell*, **54**, 5–16.